DOI: 10.37190/ABB-02484-2024-04

Influence of heat treatment method on selected physicochemical and biological properties of fluoride-substituted calcium apatite

Sylwia Zawislak[1], Joanna Rutkowska[1], Marta Trzaskowska[2], Krzysztof Palka[3], Leszek Borkowski[1*]

[1]Medical University of Lublin, Department of Biochemistry and Biotechnology, Lublin, Poland
[2]Medical University of Lublin, Independent Unit of Tissue Engineering and Regenerative Medicine, Lublin, Poland
[3]Lublin University of Technology, Faculty of Mechanical Engineering, Lublin, Poland

[*]Corresponding author: Leszek Borkowski, Medical University of Lublin, Lublin, Poland, e-mail address: leszek.borkowski@umlub.pl

Submitted: 19th July 2024
Accepted: 28th October 2024

ABSTRACT

Purpose

The synthesis of fluoridated apatite consists of several stages, among which the heat treatment has a significant impact on the physical and chemical properties. The present study aims to elucidate the influence of two different sintering methods on fluoride-substituted apatite properties.

Methods

For this purpose, a two F-substituted apatites were produced by heat treatment in different ways called “rapid sintering” and “slow sintering”. Physicochemical properties of the obtained materials were analyzed using infrared spectroscopy, scanning electron microscopy with energy dispersive spectrometry, X-ray diffraction, and mercury intrusion porosimetry. Cytotoxicity of materials was assessed using MTT test.

Results

Sintering conditions significantly influenced some porosity parameters of the materials. The samples subjected to “rapid sintering” showed a larger total pore area and mercury intrusion volume, while the samples subjected to “slow sintering” showed higher average pore diameter. Other porosity parameters did not differ significantly between the tested materials. The crystalline phases and chemical compositions of both materials were the same. Both materials appeared to be non-toxic since their extracts did not caused reduction in the viability of MC3T3-E1 cells compared to control cells and the results obtained were similar for both materials.

Conclusions

Sintering is an important step in the apatite synthesis process. The way apatite is sintered is a factor that influences its physicochemical properties. The study performed on fluoride-substituted apatite showed that sintering conditions influenced some porosity parameters but had no effect on composition, chemical structure or crystalline phase. The cytotoxicity of both materials was at the same level, indicating that both were non-toxic.

KEYWORDS

apatite properties, calcium phosphate, fluorapatite, sintering conditions,

INTRODUCTION

Hydroxyapatite (HAP) is one of the most important component of bone tissue. It builds tooth hard tissues, bones of vertebrates and some invertebrates and pathology calcified tissues like urinary calculi [27]. Synthesized bioceramics are widely used in regenerative medicine, mainly for filling bone defects [9]. They

are applied through surgeries as bioactive materials [12]. Moreover apatites are useful in dental surgeries as coatings of dental implants, addition for toothpastes and more [21]. Material used in refilling defects of bone tissues should not only be durable but also interact with bone cells, therefore, promising apatite implants have to be porous. Optimal sizes of pores are not clearly verified, some research show that the most efficient sized are about 300-400 μm which results in a large amount of bone tissue formed [36]. While other claim that it is important to be in the range of 100-200 μm, as too large pores can lead to osteon development, while too small lead to the poor integration of the material with the bone. [14,30].

HAP can be subjected to various modifications by substituting another ions in place of the hydroxyl groups, changing its properties to some extent. Comparison of hydroxyapatite and fluorapatite shown that fluoride ions substitution decreased apatite solubility and increased its chemical stability. By exchanging the hydroxyl ion (OH^-) with the fluoride ion (F^-), the stability of apatite translates into lower acid solubility, which is quite an important factor in protecting e.g. tooth enamel against caries [11,33]. The aim of developing a fluorinated biomaterial is to achieve greater mechanical strength, which significantly distinguishes it from hydroxyapatite. What is more, fluoridated apatite has a positive impact on osteoblastic proliferation, differentiation, their functional activity and increase level of alkaline phosphatase (ALP) activity [17,40].

Synthetic apatites for biomedical application can be produced by various methods [5,7,13]. In this work, we focus on the co-precipitation method, which was used for the synthesis of the studied apatites. In this method, apatite precursor is typically sintered in furnace up to 900 ºC. Further heating of the apatite above 1000 °C would lead to its dehydration into the tricalcium phosphate (TCP) phase. Tredwin et al., proved that the temperature, as well as the concentration of fluoride ions in apatite, affects dissolution rate. Also noted that the higher the heating, the smaller the amount of released Ca^{2+} and PO_4^{3-} ions. Such a decrease in the dissolution rate of an apatite driven by the temperature to which the apatite has been heated might be explained by the structural stability (higher crystallinity and lower the crystal size) of the HA/FHA/FA discs. In terms to F-substitution, the more fluoride, the slower the dissolution rate of apatite [34]. The fluoride ion is smaller than the hydroxyl one, this provides the molecule with a more compact and ordered structure which results in higher viscosity and lower the crystallization temperature. Moreover, there is a correlation between the porosity of a material and dissolving ability, due to the fact that solubility depends on the surface area, which in turn is related to the porosity of the material. It was also proven that porosity of implants may affect drug release, therefore every material should be tested for chemical reactivity [28].

In this study, fluoride-doped apatite precursor was synthesized and sintered at 800 ºC under two various conditions to verify how its physical, chemical and biological properties will be influenced. We used 2 different approaches to sintering the apatite. In the first, the apatite precipitate was placed in an

unheated muffle furnace (at room temperature, RT) and then gradually heated to a given temperature. After a given sintering period, the material was cooled in the furnace. In this approach, the material was avoided from being subjected to a large temperature difference (*"slow sintering"*). In the second approach, the material was placed in a previously heated furnace at high temperature (800 ºC), and after a given sintering period, it was removed from the hot furnace to cool at RT. In this approach, the material was subjected to a large temperature difference, which resulted in sudden, rapid and exponential sintering (*"rapid sintering"*). Both materials were then analyzed to determine the influence of sintering conditions on the material properties. Physicochemical and microstructural properties were evaluated by X-ray crystallography (XRD), scanning electron microscope coupled with energy dispersive spectroscopy (SEM-EDS), Fourier-transform infrared spectroscopy (FTIR), and mercury intrusion porosimetry (MIP). The study of biological properties included determining the cytotoxicity of the materials against MC3T3-E1 preosteoblasts.

2. MATERIAL AND METHODS

2.1. Preparation of research material

Fluoride-substituted apatite granules were synthesized in laboratory of Chair and Department of Biochemistry and Biotechnology (Medical University of Lublin, Poland) according to the procedure described in Polish Patent no. 235803 [2]. Briefly, material was synthesized by the co-precipitation method using the following reagents: calcium hydroxide ($Ca(OH)_2$; Acros Organics, Spain), orthophosphoric acid (H_3PO_4; Chempur, Poland) and sodium fluoride (NaF; Chempur, Poland). Apatite precursor was dried at 37 °C for 24 h and then at 90 °C for another 24 h. Finally, precipitated material was divided into 3 parts that have been treated in different methods (**Figure 1**).

During study, materials were labelled and treated as follows:

FAP-0 – precipitate stored at room temperature (RT), not sintered.

FAP-G – the furnace was heated to 800 ºC, then the precipitate was placed in it and heat treated for 2 hours. Then the material was removed to cool on the table at room temperature - we have named this method as *"rapid sintering".* This material was sintered according to method described in Polish Patent no. 235803 [2].

FAP-Z – the sintering was made at 800 ºC using a heating rate of 200 ºC/h with 3 hours residence time at 800 ºC, followed by natural cooling inside the furnace - we have named this method as *"slow sintering".* This method was chosen based on our own research due to the good biological properties (low cytotoxicity) of the obtained material.

Sintered ceramics were crushed in a mortar and sieved in order to obtain granules with a diameter in range of 0.2- 0.3 mm. In order to wash off the apatite dust from the surface of the granules, they were rinsed in deionized water and dried at 37 °C.

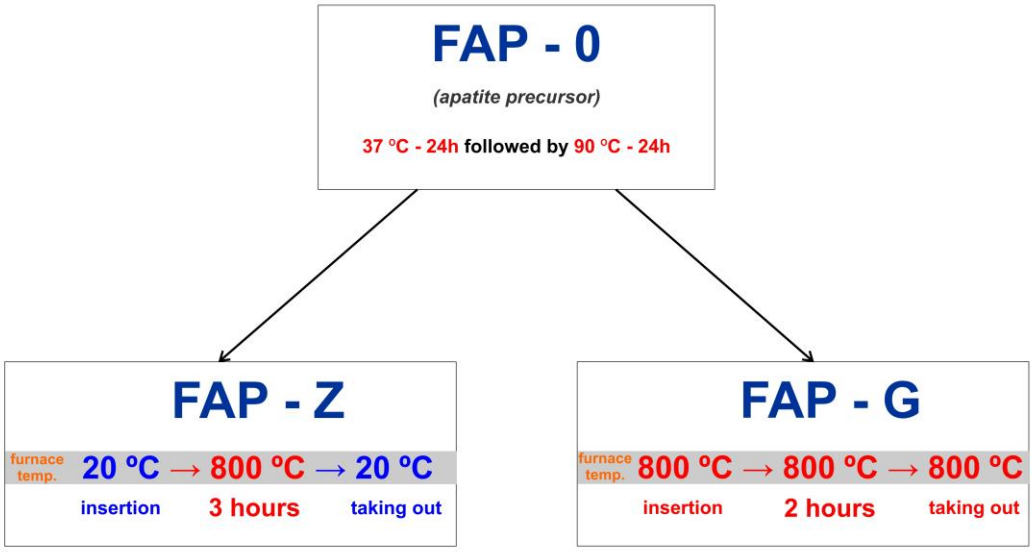

Figure 1. Scheme of temperature treatment of fluoridated apatite

2.2. Characterization of granules

2.2.1. SEM-EDS evaluation

SEM images were obtained using Nova NanoSEM 450 (FEI) in low and high vacuum conditions. The EDS analysis were taken from the whole visible area of the specimen and the chemical analysis were accomplished at the acceleration voltage of 5 kV, using the Octane Pro detector (Edax, UK).

The chemical composition (presented in atomic % and mass %) was calculated automatically by software on the basis of EDS spectra. The results from four independent repeats (n=4) were expressed as mean values ± standard deviation (SD).

2.2.2. FTIR analysis

The FTIR-ATR spectra (diamond crystal) were obtained using an IR spectrometer model Vertex 70 (Bruker Corporation, Billerica, MA, USA), 64 scans, 4 cm^{-1} resolution. Data were analyzed by the Opus 7.0 software (Bruker Corporation, Billerica, MA, USA).

2.2.3. XRD analysis

X-ray diffraction data were acquired using the HZG-4 diffractometer (Carl Zeiss, Germany) equipped with conventional X-ray tube with copper anode (operated at 40 kV and 20 mA) and Ni filter applied. The X-ray tube, sample and detector were positioned in a Bragg-Brentano geometry. Diffraction

data were collected by step counting in the range $2\Theta = 20 \div 50°$ at 0.01 deg. intervals for 2 seconds per data point. Identification of phases contained in tested materials were done using the PDF-4 database (ICDD, USA) based on diffraction patterns.

2.2.4. Determination of pore size distribution by mercury porosimetry

The most frequent porosimetric parameters were measured according to the ISO 15901-1:2005 standard with Autopore IV 9500 mercury porosimeter (Micrometrics Inc., Norcross, GA, USA). Before the experiment, the samples were dried at 37 ºC. Mercury intrusion was performed at pressures up to 228 MPa. The range of the examined pores was 5 nm to 360 μm. Statistically significant results were considered at $p < 0.05$ according to an unpaired t-test (GraphPad Prism 7.04 Software, San Diego, CA, USA).

2.3. Cytotoxicity assessment - in vitro cell culture test

In vitro cytotoxicity studies were conducted using a mouse calvarial preosteoblast cell line (MC3T3-E1 Subclone 4; ATCC-LGC, standards, Teddington, UK). Cells were cultured in Minimum Essential Medium alpha (MEM alpha) (Gibco, Life technologies, Carlsbad, CA, USA) supplemented with 10% fetal bovine serum (FBS; Pan-Biotech GmbH, Aidenbach, Bavaria, Germany) and antibiotics: 100 U/mL penicillin (Sigma-Aldrich Chemicals, Warsaw, Poland) and 0.1 mg/mL streptomycin (Sigma-Aldrich Chemicals, Warsaw, Poland). Cells were cultured at 37 ºC with 5% CO_2 in air atmosphere.

The test assessing the cytotoxicity of biomaterials was performed in indirect contact with the material according to the ISO 10993-5 (2009) standard [29]. The experiment used liquid extracts of the biomaterials, obtained by incubating 100 mg of granules in 1 ml of complete culture medium for 24 hours at 37°C. The cells were seeded at a density of 2×10^4 cells per well in the culture medium, into a 96-well plate and then cultured for 24 hours. After this time, the medium was replaced with the appropriate biomaterial extract, and the cells were cultured for another 24 or 48 hours. Cell viability was determined using the MTT test according to the procedure described in the previous article [24]. The test results were presented as a percentages of the absorbance value obtained for the control. The experiment was performed in three independent replicates. The determination of statistical differences was made using one-way analysis of variance (One-way ANOVA) with Tukey's post hoc test (GraphPad Prism 7.04 Software, San Diego, CA, USA).

3. RESULTS

SEM images of FAP-0, FAP-Z and FAP-G samples were presented in **Figure 2**. The surface of the samples FAP-Z and FAP-G was significantly different from the rough surface of the sample FAP-0, while the samples FAP-Z and FAP-G were smooth, homogeneous and not very different from each other.

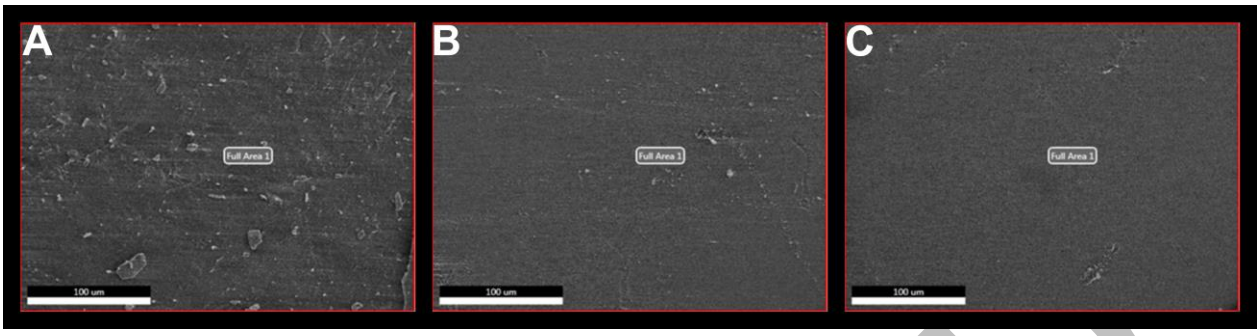

Figure 2. SEM micrographs of samples: A) FAP-0, B) FAP-Z, and C) FAP-G.

According to EDS analysis (**Figure 3**), apatites FAP-Z and FAP-G contained comparable amounts of calcium (Ca), phosphorus (P), oxygen (O), and fluoride (F) while non-sintered FAP-0 contained significantly higher amount of O and F, and lower amount of Ca. P content has been found to be insignificantly higher in FAP-G and statistically significantly higher ($P < 0.05$) in FAP-Z compared to FAP-0 (**Fig. 3A**).

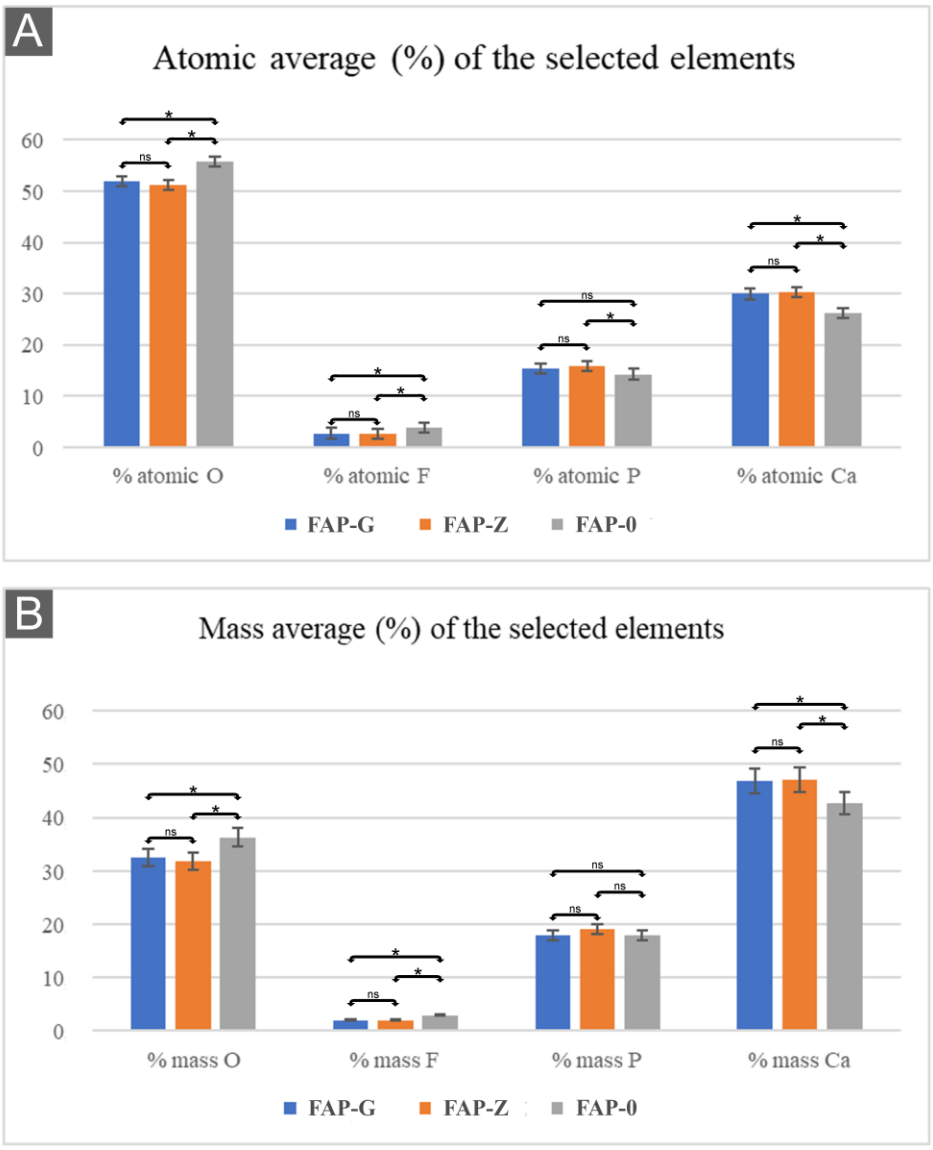

Figure 3. Elemental content of tested apatites based on EDS analysis. Composition of materials was expressed as percentage of elements by atoms (A) and masses (B). Statistically significant differences in the element content between different materials according to One-way ANOVA followed by Tukey´s test (P <0.05) were indicated with *, ns – no significant.

Figure 4 shows the FTIR spectra of fluoride-substituted apatite which was heated at 800 ºC (FAP-Z and FAP-G) and non-heated (FAP-0). In FAP-0 strong bands of phosphate groups observed at 561 cm^{-1}, 603 cm^{-1} and 964 cm^{-1}, 1024 cm^{-1}, 1091 cm^{-1}, low intensity peaks of carbonate groups were identified at 1458 cm^{-1}, 1419 cm^{-1} and 873 cm^{-1}, and vibration assigned to H_2O was found as wide band near 3470 cm^{-1}. In FAP-Z and FAP-G phosphate bands were observed as above, CO_2 peaks were in the same positions but

had lower intensity, while presence of OH^- groups was demonstrated at 679 cm^{-1} and 3539 cm^{-1}. Moreover, sintered apatites differed from FAP-0 by the presence of a peak at 744 cm^{-1} assigned to F^-.

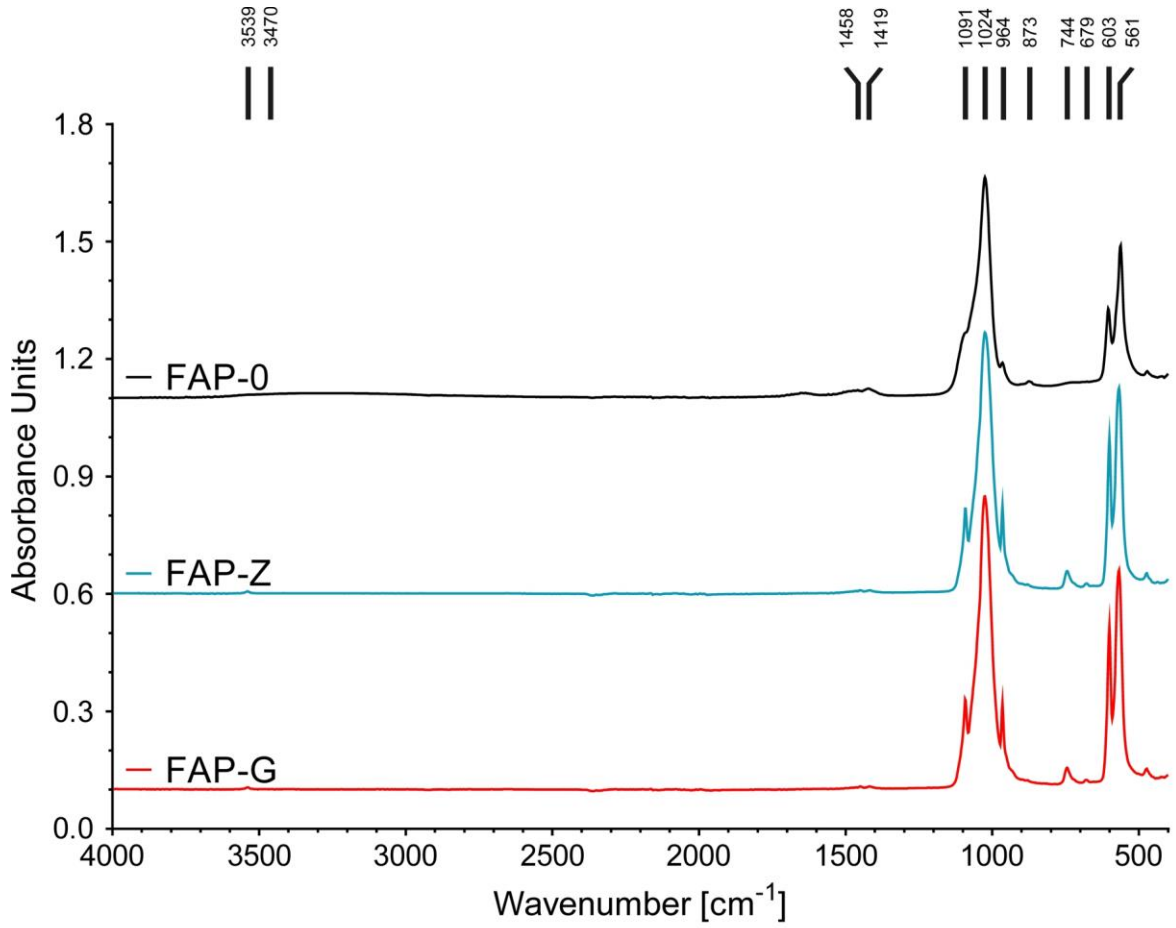

Figure 4. FTIR spectra of samples: FAP-0, FAP-Z, and FAP-G in the range 400-4000 cm^{-1}.

The phase composition of tested samples and two standard ceramics: fluorapatite (FAP) and hydroxyapatite (HAP) assessed by the XRD technique was presented in **Figure 5**. It shows that the peeks of fluoride-substituted ceramics (all tested samples: FAP-0, FAP-Z, FAP-G) are shifted to the higher 2theta values in relation to the HAP standard (ICDD 00-055-0592), and at the same time, their positions are following the data of the FAP standard (ICDD 01-080-8486). No peaks from other substances were found which indicates the presence of pure fluorapatite in tested materials. The shape of the XRD pattern for the FAP-0 sample indicates the small crystallinity size (8.55 nm) due to the lack of thermal treatment in contrast to over 50 nm for sintered ones.

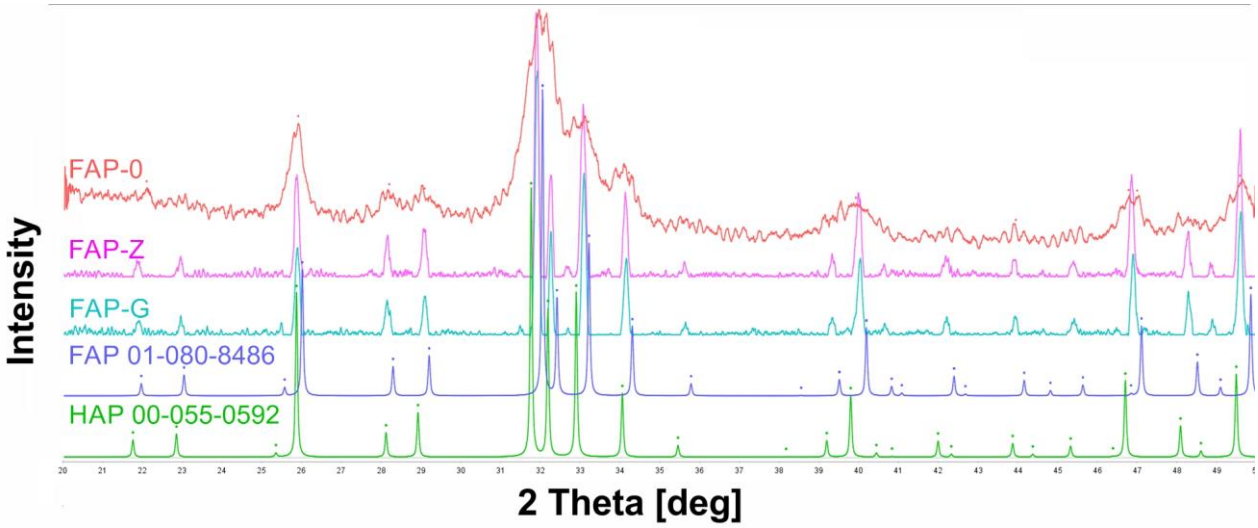

Figure 5. Summary of results of X-ray crystallography of samples FAP-0, FAP-Z, FAP-G and two standards-hydroxyapatite and fluorapatite.

The results obtained with the mercury intrusion using mercury porosimeter are shown in the **Table 1**. Statistical analysis of the results revealed that there was no difference in porosity, bulk density, apparent density, and median pore diameter between the FAP-Z and FAP-G samples. However, sample FAP-G exhibited higher total intrusion volume and total pore area in relation to sample FAP-Z. Lower total pore area in sample FAP-Z was associated with a larger pore diameter in comparison to sample FAP-G.

Table 1. Summary of mercury porosimetry results

	FAP - G		FAP - Z		statistically significant difference *
Parameters	mean	SD	mean	SD	
Total intrusion volume [cm^3/g]	**0.87**	0.003	**0.85**	0.001	*yes*
Total pore area [m^2/g]	**6.63**	0.060	**5.45**	0.020	*yes*
Bulk density [g/cm^3]	**0.82**	0.000	**0.84**	0.000	*no*
Apparent (skeletal) density [g/cm^3]	**2.89**	0.000	**2.9**	0.007	*no*
Porosity [%]	**71.49**	0.080	**71.1**	0.110	*no*
Median pore diameter (volume) [µm]	**48.83**	1.020	**54.09**	1.850	*no*
Median pore diameter (area) [µm]	**0.20**	0.000	**0.23**	0.000	*no*
Average pore diameter [µm]	**0.52**	0.007	**0.62**	0.007	*yes*

** statistically significant differences between samples according to unpaired Student's t-test at $P < 0.05$*

Cytotoxicity of the granules was assessed using a colorimetric MTT test. The ISO 10993-5 (2009) standard indicates that the biomaterial is considered non-toxic if cell viability after incubation with the biomaterial extract is above 70% of the control cells. In our study, both tested biomaterials were non-toxic to mouse preosteoblasts (MC3TC-E1 cell line). Cell viability after both 24 and 48 hours of exposure to biomaterial extracts exceeded 100% of the control (**Figure 6**). Viability of cells after 24 hour incubation with samples extracts was significantly higher than control cells (**Figure 6A**). After 48h, the results for FAP-G and FAP-Z were at the same level as for control cells (**Figure 6B**).

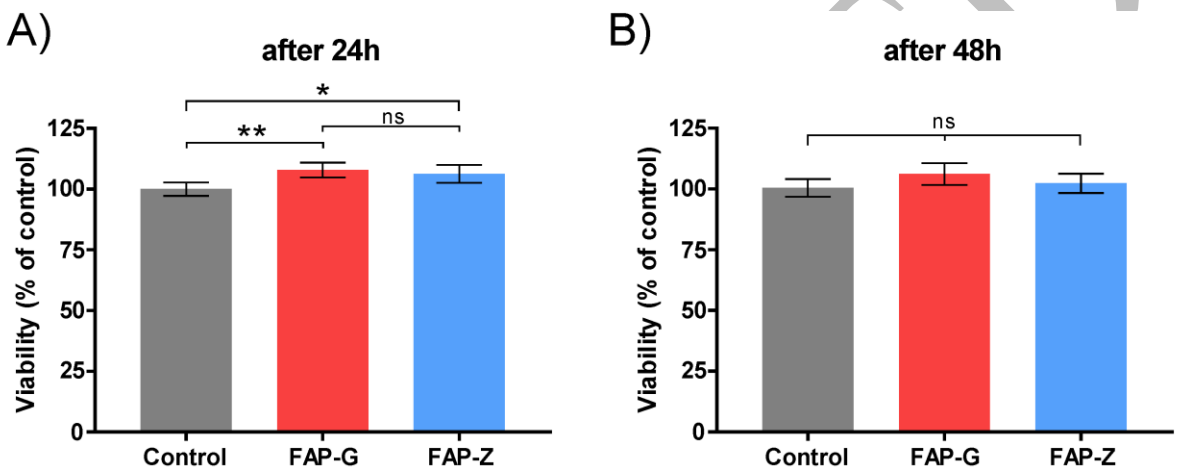

Figure 6. MTT cytotoxicity test performed for the biomaterials using mouse preosteoblasts (MC3TC-E1 cell line) according to ISO 10993-5 standard. The results of statistical analysis using the One-way ANOVA test followed by Tukey's multiple comparison test were as follows: * p=0.032, ** p=0.009, ns = p>0.05.

4. DISCUSSION

Many apatites (calcium phosphates) are used in industry, medicine and scientific research. These include hydroxyapatite, fluorapatite, chlorapatite, carbonate apatite and others. They can be of either natural or synthetic origin. It is known that the final properties of artificial apatites are influenced by the conditions of synthesis, such as: synthesis method, type of reagents, solution pH, temperature, time, mixing, etc. One of the last stages of apatite synthesis is sintering, i.e. procedure conducted in to improve the characteristics of the starting materials. This process involves heating at high temperatures and alter the physico-chemical characteristics of the initial powders and affect their surface reactivity, which translates into the biological properties of the material [15,25]. For this reason, it is so important to determine the effect of sintering conditions on the final properties of apatite. So far, studies have been conducted on the sintering dwell time [19] and sintering temperature of the apatite precursor [16,35]. The aim of this study was to compare two

different approaches to the apatite sintering process, which we called "fast sintering" and "slow sintering". Rapid sintering means that the samples were placed in a furnace heated to the target temperature and immediately removed to room temperature after the sintering process. Slow sintering means that the samples were placed in a non-heated furnace (room temperature), then heated at a selected rate until the target temperature was reached and sintered for a specified time. Based on the literature review, it can be stated that the slow sintering method is used in the vast majority, while the rapid method is rarely used. However, it is impossible to determine the sintering method in every case, because the apatite sintering process is not always precisely described in the publication.

In our study, the research material was fluorapatite sintered at 800 °C and the reference material was unsintered fluorapatite (FAP-0). We labelled the rapid sintering material as FAP-G and the slow sintering material as FAP-Z. XRD, SEM and EDS analysis did not show any differences between FAP-G and FAP-Z. Both materials had a smooth and homogeneous surface and showed no significant statistical differences in elemental composition. FAP-G and FAP-Z had higher Ca and P content than the FAP-0 material and lower O content, which is most likely due to water evaporation sintering at 800 ºC and its loss from the structure of apatite [1,22].

The FTIR analysis showed no differences between the FAP-Z and FAP-G materials, while the FAP-0 material showed significant differences in relation to the sintered apatites. The first difference between the sintered materials and unsintered FAP-0 was the presence of a peak at 744 cm^{-1} assigned to F^- [26]. Phosphate bands in FAP-Z and FAP-G have largely increased in intensity (became narrow and sharp) due to increased crystallinity of apatite structure which is typical for sintered apatites as observed by other authors [6,20]. Bands assigned to CO_2 groups were detected in all tested materials, however, had lower intensity in sintered materials. Carbonate peaks at 1458 cm^{-1}, 1419 cm^{-1} and 873 cm^{-1} suggest type B substitution (CO_3^{2-} replacing PO_4^{3-}) [10]. Bands located at wavenumbers of ~3470 cm^{-1} in FAP-0 and at ~3539 cm^{-1} in sintered apatites were assigned to H_2O (OH) because water absorption bands of apatite typically produce bands at wavenumbers between ~3600 cm^{-1} and 3400 cm^{-1} [8,31]. However, it is likely that the peak at 3539 cm^{-1} represents the absorption of OH-F vibration band that is often found at position ~3533 cm^{-1} [10,26,31,32,38]. Further studies performed in this region and at higher resolution would allow distinguishing OH-OH from OH-F vibrations as done by Hammerli et al. [10]. Disappearance of the large band of H_2O at 3470 cm^{-1} suggest evaporation of crystalline water in apatite powders during the sintering process which is consistent with our EDS results and with the observations of Xu et al. [39].

It is known that sintering process significantly influences the microstructure of the apatite [35]. Several studies have been carried out to show the effect of sintering conditions on HAP [4,16,18,23,37] and FAP microstructure [3,4]. The results obtained in these studies show that the increase/decrease of sintering temperature significantly affects the density, porosity and specific surface area of apatite. In our study,

fluorapatites produced by rapid sintering and slow sintering showed similar porosity and density, however, they differed statistically significantly in the total intrusion volume, total pore area, average pore diameter. The obtained results indicate that by changing the approach to apatite sintering it is possible to control some microstructural parameters without significantly affecting the density and porosity of the material.

In summary, the only differences we observed between the two fluorapatites sintered by different methods concern only some microstructure parameters. These changes did not have a significant effect on the cytotoxicity of FAP, which was high in both cases. This study shows that not only the temperature and time of sintering affect the properties of the final material, but also whether the apatite precursor is placed in a "hot" or "cold" furnace. The presented results can be helpful in the work on apatite materials with the desired chemical, physical and biological properties.

5. CONCLUSIONS

In this study we investigated the influence of sintering conditions of fluoride-doped apatite on its physical properties, chemical composition, phase composition and biological properties. On the basis of the obtained results, it can be concluded that:

1. Sintering method (time and conditions of heat treatment) have affected some (but not all) of the porosity parameters, i.e. total intrusion volume, total pore area, and average pore diameter. However, porosity, bulk density, apparent density, and median pore diameter were at the same level.
2. The sintering method had no significant effect on the composition, chemical structure and phase composition of fluorinated ceramics, which was confirmed by EDS, FTIR and XRD.
3. Cell viability measured by ISO 10993-5:2009 standard was very high for both materials indicating that they were non-toxic and there was no significant difference between materials.
4. Both sintering methods caused evaporation of crystalline water.

As shown in this study, the conditions of apatite ceramics synthesis influence certain physicochemical parameters. In-depth knowledge of the mechanism of chemical and structural changes taking place in ceramics during the sintering process will allow to obtain a product with the desired parameters, which will be reflected in its biological properties and its potential application in orthopedics and dental surgery.

6. ACKNOWLEDGMENT

This research was funded by the Ministry of Science and Higher Education in Poland within project of the Medical University of Lublin (DS. 6 and DS. 630) and by the Medical University of Lublin within Young Scientists Program awarded to Leszek Borkowski (MNmb3). The paper was also supported by

Ministry of Education and Science in Poland within the discipline fund of Lublin University of Technology (grant FD-20/IM-5/078).

7. REFERENCES:

1. Belamri D., Harabi A., Karbouaa N., Benyahia N., The effect of KF on the structural evolution of natural hydroxyapatite during conventional and microwave sintering, Ceram Int, 2020, 46(1):1189-1194.
2. Borkowski L., Belcarz A., Przekora A., Ginalska G., Production Method for Biocompatible Implant Material. Polish Patent no. 235803, 6 October 2020.
3. Borkowski L., Przekora A., Belcarz A., Palka K., Jozefaciuk G., Lübek T., Jojczuk M., Nogalski A., Ginalska G., Fluorapatite ceramics for bone tissue regeneration: Synthesis, characterization and assessment of biomedical potential, Mater Sci Eng C, 2020, 116:111211.
4. Chaari K., Ayed F.B., Bouaziz J., Bouzouita K., Elaboration and characterization of fluorapatite ceramic with controlled porosity, Materials Chemistry and Physics, 2009, 113(1):219-226.
5. El-Gendy N.S., El-Salamony R.A., Younis S.A., Green synthesis of fluorapatite from waste animal bones and the photo-catalytic degradation activity of a new ZnO/green biocatalyst nano-composite for removal of chlorophenols, J Water Process Eng, 2016, 12:8-19.
6. Etok S.E., Valsami-Jones E., Wess T.J., Hiller J.C., Maxwell C.A., Rogers K.D., Manning D.A.C., White M.L., Lopez-Capel E., Collins M.J., Buckley M., Penkman K.E.H., Woodgate S.L., Structural and chemical changes of thermally treated bone apatite, J Mater Sci, 2007, 42(23):9807-9816.
7. Fathi M.H., Zahrani E.M. Fabrication and characterization of fluoridated hydroxyapatite nanopowders via mechanical alloying, J Alloys Compd, 2009, 475(1-2):408-414.
8. Freund F., Knobel R.M., Distribution of fluorine in hydroxyapatite studied by infrared spectroscopy, J Chem Soc Dalton Trans, 1977, 11:1136-1140.
9. Ghiasi B., Sefidbakht Y., Mozaffari-Jovin S., Gharehcheloo B., Mehrarya M., Khodadadi A., Rezaei M., Ranaei Siada S.O., Uskoković V., Hydroxyapatite as a biomaterial–a gift that keeps on giving, Drug Dev Ind Pharm, 2020, 46(7):1035-1062.
10. Hammerli J., Hermann J., Tollan P., Naab, F., Measuring in situ CO2 and H2O in apatite via ATR-FTIR, Contrib Mineral Petrol, 2021, 176:1-20.
11. Klimuszko E., Sierpińska T., Gołębiewska M., Construction of enamel and its resistance to pathological factors. A literature review, Prosthodontics, 2015, 65(3):241-251.
12. Kokubo T., Bioceramics and their Clinical Applications, Woodhead Publishing Series in Biomaterials, CRC Press, 2008.

13. Kurmaev E.Z., Matsuya S., Shin S., Watanabe M., Eguchi R., Ishiwata Y., Takeuchi T., Iwami M., Observation of fluorapatite formation under hydrolysis of tetracalcium phosphate in the presence of KF by means of soft X-ray emission and absorption spectroscopy, J Mater Sci-Mater M, 2002, 13(1):33-36.
14. Laska A., Biomateriały stosowane w inżynierii tkankowej do regeneracji tkanek, Zeszyty Naukowe Towarzystwa Doktorantów Uniwersytetu Jagiellońskiego. Nauki Ścisłe, 2017, 14:187-196.
15. LeGeros R.Z., Biodegradation and bioresorption of calcium phosphate ceramics, Clin Mater, 1993, 14(1):65-88.
16. Malina D., Biernat K., Sobczak-Kupiec A., Studies on sintering process of synthetic hydroxyapatite, Acta Biochim Pol, 2013, 60(4):851-855.
17. Nakade O., Koyama H., Arai J., Ariji H., Takada J., Kaku T., Stimulation by low concentrations of fluoride of the proliferation and alkaline phosphatase activity of human dental pulp cells in vitro, Arch Oral Biol, 1999, 44:89-92.
18. Obada D.O., Dauda E.T., Abifarin J.K., Dodoo-Arhin D., Bansod N.D., Mechanical properties of natural hydroxyapatite using low cold compaction pressure: Effect of sintering temperaturę, Mater Chem Phys, 2020, 239:122099.
19. Obada D.O., Idris N., Idris M., Dan-Asabe B., Salami K.A., Oyedeji A.N., Csaki S., Sowunmi A.R., Abolade S.A., Akinpelu S.B., Akande A., The effect of sintering dwell time on the physicochemical properties and hardness of hydroxyapatite with insights from ab initio calculations, CSCEE, 2024, 9:100648.
20. Ooi C.Y., Hamdi M., Ramesh S., Properties of hydroxyapatite produced by annealing of bovine bone, Ceram Int, 2007, 33(7):1171-1177.
21. Pajor K., Pajchel L., Kolmas J., Hydroxyapatite and Fluorapatite in Conservative Dentistry and Oral Implantology - A Review, Materials, 2019, 12(17):2683.
22. Poovendran K., Wilson K.J., Amalgamation and characterization of porous hydroxyapatite bio ceramics at two various temperatures, Mater Sci Semicond Process, 2019, 100:255-261.
23. Prokopiev O., Sevostianov I., Dependence of the mechanical properties of sintered hydroxyapatite on the sintering temperaturę, Mater Sci Eng A, 2006, 431(1-2):218-227.
24. Przekora A., Czechowska J., Pijocha D., Ślósarczyk A., Ginalska G., Do novel cement-type biomaterials reveal ion reactivity that affects cell viability in vitro?, Open Life Sci, 2014, 9(3):277-289.
25. Rey C., Maturation of poorly crystalline apatites: chemical and structural aspects in vivo and in vitro, Cells and Mater, 1995, 5:345-356.

26. Rintoul L., Wentrup-Byrne E., Suzuki S., Grøndahl L., FT-IR spectroscopy of fluoro-substituted hydroxyapatite: strengths and limitations, J Mater Sci Mater Med, 2007, 18:1701-1709.
27. Slosarczyk A., Biomateriały ceramiczne, Biocybernetyka i Inżynieria Biomedyczna. In: Blazewicz S., Stoch L., Biomateriały, AOW EXIT, 2003.
28. Slosarczyk A., Szymura-Oleksiak J., Mycek B., The kinetics of pentoxifylline release from drug-loaded hydroxyapatite implants, Biomaterials, 2000, 21:1215-1221.
29. Standard ISO 10993-5:2009. Biological Evaluation of Medical Devices—Part5: Tests for In Vitro Cytotoxicity; International Organization for Standardization: Geneva, Switzerland, 2009.
30. Szczepkowska M., Łuczuk M., Porous materials for the medical applications, Syst Wspomagania Inzynierii Prod, 2014, 2:231-239.
31. Tacker R.C., Hydroxyl ordering in igneous apatite, Am Min, 2004, 89(10):1411-1421.
32. Taheri M.M., Kadir M.R.A., Shokuhfar T., Hamlekhan A., Assadian M., Shirdar M.R., Mirjalili A., Surfactant-assisted hydrothermal synthesis of fluoridated hydroxyapatite nanorods, Ceram Int, 2015, 41(8):9867-9872.
33. Telesiński A., Śnioszek M., Bioindykatory zanieczyszczenia środowiska naturalnego fluorem, Bromatol Chem Toksyk, 2009, 42(4):1148-1145.
34. Tredwin C.J., Young A.M., Abou Neel E.A., Georgiou G., Knowles J.C., Hydroxyapatite, fluor-hydroxyapatite and fluorapatite produced via the sol–gel method: dissolution behaviour and biological properties after crystallisation, J Mater Sci-Mater M, 2014, 25(1):47-53.
35. Trzaskowska M., Vivcharenko V., Przekora A., The impact of hydroxyapatite sintering temperature on its microstructural, mechanical, and biological properties, I J Mol Sci, 2023, 24(6):5083.
36. Tsuruga E., Takita H., Itoh H., Wakisaka Y., Kuboki Y., Pore Size of Porous Hydroxyapatite as the Cell-Substratum Controls BMP-Induced Osteogenesis, J Biochem, 1997, 121(2):317-324.
37. Wang A.J., Lu Y.P., Zhu R.F., Li S.T., Xiao G.Y., Zhao G.F., Xu W.H., Effect of sintering on porosity, phase, and surface morphology of spray dried hydroxyapatite microspheres, J Biomed Mater Res A, 2008, 87(2):557-562.
38. Wirtu Y.D., Melak F., Yitbarek M., Astatkie H., Aluminum coated natural zeolite for water defluoridation: a mechanistic insight, Groundw Sustain Dev, 2021, 12:100525.
39. Xu Z., Qian G., Feng M., Using polyacrylamide to control particle size and synthesize porous nano hydroxyapatite, Results Phys, 2020, 16:102991.
40. Yoon B.H., Kim H.W., Lee S.H., Bae C.J., Koh Y.H., Kong Y.M., Kim H.E., Stability and cellular responses to fluorapatite-collagen composites, Biomaterials, 2005, 26(16):2957-2963.